sustainability

MDPI

Article

Spatial Coupling Characteristics Between Tourism Point of Interest (POI) and Nighttime Light Data of the Changsha–Zhuzhou–Xiangtan Metropolitan Area, China

Jiangzhou Wu [1,2], Qing Zhang [1,2,*] and Zhida Li [3]

[1] College of National Park & Tourism, Central South University of Forestry and Technology, Changsha 410004, China; jiangzhou.wu@csuft.edu.cn
[2] National Forestry and Grassland Engineering Research Center for Forest Tourism, Changsha 410004, China
[3] Graduate School of Business Administration, Keio University, Tokyo 223-8526, Japan; lizhida126@keio.jp
* Correspondence: qing@csuft.edu.cn; Tel.: +86-137-2385-9696

Abstract: Metropolitan areas, as pivotal hubs for global tourism and economic growth, necessitate sustainable spatial planning to balance development with ecological preservation. As critical geospatial datasets, nighttime light (NTL) and point of interest (POI) data enable the robust analysis of urban structural patterns. Building upon coupling coordination theory and polycentric spatial frameworks, this study investigates the spatial interdependencies between tourism POI and NTL data in China's Changsha–Zhuzhou–Xiangtan Metropolitan Area (CZTMA). Key findings reveal high spatial coupling homogeneity, with three urban cores exhibiting radial value attenuation from city centers toward the tri-city intersection; concentric zonation patterns where NTL-dominant rings encircle high-coupling nuclei, contrasting with sporadic POI-intensive clusters in peri-urban towns; and sector-specific luminosity responses, where sightseeing infrastructure demonstrates the strongest localized NTL impacts through multiscale geographically weighted regression (MGWR). These findings establish a novel "data fusion-spatial coupling-governance" analytical framework and provide actionable insights for policymakers to harmonize tourism-driven urbanization with ecological resilience, contributing to United Nations Sustainable Development Goal (SDG) 11 (Sustainable Cities).

Keywords: nighttime light; point of interest; tourism spatial structure; coupling analysis; Changsha–Zhuzhou–Xiangtan Metropolitan Area

check for updates

Academic Editor: Seul Ki Lee

Received: 29 January 2025
Revised: 1 March 2025
Accepted: 6 March 2025
Published: 9 March 2025

Citation: Wu, J.; Zhang, Q.; Li, Z. Spatial Coupling Characteristics Between Tourism Point of Interest (POI) and Nighttime Light Data of the Changsha–Zhuzhou–Xiangtan Metropolitan Area, China. *Sustainability* **2025**, *17*, 2391. https://doi.org/10.3390/su17062391

Copyright: © 2025 by the authors. Licensee MDPI, Basel, Switzerland. This article is an open access article distributed under the terms and conditions of the Creative Commons Attribution (CC BY) license (https://creativecommons.org/licenses/by/4.0/).

1. Introduction

Metropolitan areas serve as the fundamental units of international competition and the primary platforms for a nation's economic and social development, playing a pivotal role in driving integrated regional development [1]. Defined as urbanized spatial systems anchored by megacities or large urban hubs with extensive radiating influence, metropolitan areas typically span a one-hour commuting radius as their functional footprint [2]. These regions integrate diverse cities of varying characteristics, scales, and hierarchies within geographically contiguous zones, underpinned by shared ecological and infrastructural foundations [3]. In China, rapid economic growth, the continuous expansion of industrial scale, and the increasingly sophisticated industrial system have effectively propelled the construction and development of metropolitan areas [4]. Emphasizing the development of modern service industries, with tourism as a key component, is essential for metropolitan areas to accelerate the transformation of economic development modes, establish a modern

industrial system, and cultivate new economic growth poles [5]. Currently, the Chinese government has approved the construction of seven metropolitan areas: Nanjing, Fuzhou, Chengdu, Changsha–Zhuzhou–Xiangtan, Xi'an, Chongqing, and Wuhan. These areas are endowed with abundant natural landscapes, historical and cultural tourism resources, and host numerous high-level tourist attractions, making them significant tourist destinations in China.

The rapid urbanization of metropolitan areas globally has intensified the need for sustainable spatial planning, particularly in balancing economic growth with environmental stewardship. The spatial organization of tourism within metropolitan systems represents a critical research frontier in regional planning [6]. The tourism spatial structure refers to the spatial organizational relationships among various elements of the tourism system, including their positions, interconnections, and interactions in space, as well as their generation, movement, and development [7]. Researchers primarily investigate the evolutionary processes, spatial structures, and formation mechanisms of tourism from a spatial perspective, uncovering the characteristic patterns and typical models of tourism space formation and evolution [8,9]. Initially, research on the spatial structure of tourism in metropolitan areas focused on individual cities, emphasizing the spatial layout, network structure, and evolutionary patterns of tourism within single cities, particularly from perspectives such as the allocation of tourism development elements and the spatial mobility of tourists [10,11]. With the rapid development of global cities, metropolitan areas such as New York, Tokyo, and Shanghai have emerged as key regions for global urban development due to their advantages in capital, technology, and talent [12]. Consequently, research on metropolitan tourism has expanded from individual cities to broader metropolitan regions. As urban tourism evolves into metropolitan tourism, various elements gradually converge, tourism formats continually evolve, and spatial relationships become increasingly complex [13]. Scott categorized the evolution of metropolitan tourism spatial structures into three stages: single-center, multi-center, and networked stages [14]. He argued that during the multi-center and networked stages, the connections and functional cooperation among centers become more pronounced. Huang suggested that the spatial effects dominated by the networked model would gradually strengthen, contributing to the formation of a balanced and open regional space [15]. Furthermore, metropolitan areas nowadays face dual challenges: leveraging tourism for economic transformation while mitigating urban sprawl and environmental degradation. Existing studies often neglect the integration of multi-source geospatial data to address these sustainability challenges, limiting their applicability in dynamic governance contexts. Therefore, studying tourism's spatial structure and its associated aggregation in metropolitan areas is crucial for optimizing the spatial structure of tourism, promoting its progression toward the multi-center networked stage, and facilitating coordinated regional development. Current research on the spatial structure of tourism in metropolitan areas encompasses the current status and optimization, evolution and influencing factors, optimization strategies, as well as spatial effects of tourism, spatial tourism behaviors, the spatial differential development of tourism, and the spatial layout of the tourism industry [16–20].

Nighttime light (NTL) data and point of interest (POI) data are invaluable for studying urban spaces [21]. These datasets are frequently employed to analyze urban patterns and urbanization, human activities and their impacts, and regional economic growth; quantify regional GDP changes and population spatialization; and estimate electricity and energy consumption [22–26]. NTL data are characterized by open data sources, rapid updates, extensive coverage, and high temporal resolution, making them widely applicable in fields such as metropolitan area expansion, urban economic and industrial development, urban evolution, and the hierarchical patterns of urban systems [27,28]. With the explosive growth

of big data, not only statistical data but also remotely sensed images and other openly accessible data are playing an increasingly significant role in research on urban structure [29]. Large-scale, high-precision positioning data enable scholars to analyze the internal spatial structure of cities from micro, macro, dynamic, and static perspectives [30]. POI data, which contain information about the spatial distribution and types of geographical features, offer advantages such as precise feature positioning, diverse feature types, and rapid data updates, representing point data of geographical entities on the ground [25,31]. Compared to traditional survey methods, POI data provide highly accurate and timely identification of urban centers. Currently, POI data are primarily used for urban boundary extraction, urban built-up area identification, urban functional area classification, and urban industrial spatial pattern analysis [32].

In recent years, research on NTL data and POI data has extended into the field of tourism research, primarily focusing on reflecting changes in urban leisure hotspots, the impact of tourism activities, and tourism spatial spillover effects [33]. However, few studies have combined NTL data and POI data to examine the spatial structure of tourism in metropolitan areas. Despite growing interdisciplinary applications, three fundamental barriers have hindered the widespread adoption of the integration of two datasets in tourism research. Firstly, the daily update frequency of POI data (e.g., Amap/Baidu Map) contrasts sharply with the monthly composite cycles of NPP-VIIRS NTL data, creating synchronization challenges for dynamic studies [25]. Secondly, POI data capture tourism facility distribution and NTL data reflect economic activity intensity; existing studies often fail to establish interpretable linkages between tourism-related POI categories and NTL luminosity gradients. Thirdly, conventional zonal statistics methods tend to overlook the modifiable areal unit problem when correlating POI density with NTL intensity, particularly in the transitional urban–rural fringe.

In order to address the above limitations, the paper extracts the potential central range through multi-scale segmentation of NTL intensity and combines it with tourism POI data to identify the multi-center distribution in the Changsha–Zhuzhou–Xiangtan Metropolitan Area (CZTMA) of China. As the only approved metropolitan area in central China, CZTMA exhibits transitional characteristics between single-core dominance (Changsha) and emerging polycentricity (Zhuzhou–Xiangtan), providing an ideal laboratory for observing metropolitan spatial restructuring. Furthermore, the area encompasses gradient urbanization zones from the urban core to the ecological preserves, enabling comprehensive analysis of correlations between the tourism industry and light intensity across development spectra. Based on tourism POI data and NTL data, the paper analyzes the tourism spatial structure of CZTMA from multiple perspectives, including functional structure identification, spatial correlation measurement, and the service range of the main center, aiming to provide insights for optimizing the tourism spatial planning of CZTMA and aligning with global sustainability agendas by demonstrating how spatially informed policies can enhance tourism's contribution to green economies, resilient infrastructure, and inclusive growth.

2. Materials and Methods

2.1. Study Area

The research area of this paper is CZTMA of Hunan Province, China. Approved for construction by the Chinese government in February 2022, CZTMA is the fourth national-level metropolitan area in China and the first in central China. Spanning a total area of 18,900 km^2, it encompasses the entire administrative region of Changsha, the urban areas of Zhuzhou and Xiangtan, and Liling, Shaoshan, and Yisuhe in Hunan Province (Figure 1). In 2021, the metropolitan area had a permanent population of 14.84 million and a GDP of

246 billion US dollars, with a per capita GDP of 16,576 US dollars, solidifying its position as the core growth engine for Hunan Province's economic and social development [34]. The three core cities of the metropolitan area (Changsha, Zhuzhou, and Xiangtan) are geographically distributed in a triangular formation along the Xiangjiang River, with the distance between the centers of any two cities being less than 50 km. The region boasts over 50 scenic spots of various types, including museums, memorial halls, forest parks, geological parks, wetland parks, and theme parks. In 2023, it attracted more than 250 million tourists, establishing itself as a significant urban tourist destination in China.

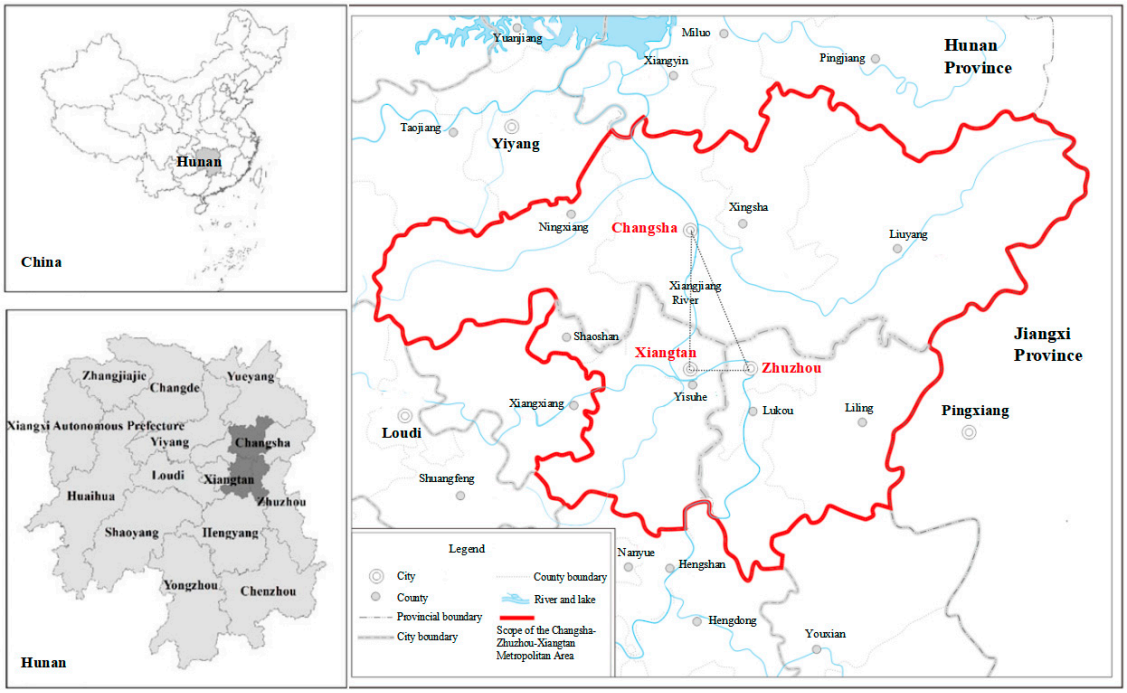


Figure 1. The location of study area.

2.2. Data Sources

2.2.1. NTL Data

The NTL data used in this study were obtained from the NPP/VIIRS dataset provided by the National Center for Environmental Information (NCEI) of the National Oceanic and Atmospheric Administration (NOAA) (https://eogdata.mines.edu/products/vnl/) (accessed on 1 March 2025). The NPP/VIIRS dataset comprises monthly light images, available in two product types: vcmcfg and vcmslcfg. Previous research indicates that the vcmcfg data offer superior quality and are more suitable for identifying changes in urban spatial structure and patterns, as they exclude data potentially affected by scattered light [35]. Therefore, this study utilizes the vcmcfg data (avg_rade9 file) for CZTMA from January to December 2023 (12 periods in total) as the primary source of NTL data. Additionally, to capture the historical dynamics of NTL changes, the study also acquired monthly average light radiation datasets and light images for the metropolitan area from 2020 to 2023. These datasets were used to calculate the sum of DN values of bright pixels (Total DN value, TDN), the maximum light intensity (DN maximum, DNmax), and the total area of NTL (Total Area, TA).

2.2.2. POI Data

The point of interest (POI) data were sourced from the Amap Open Platform. The platform categorizes POI data into three tiers—major, middle, and minor categories—encompassing 23 major categories, 267 middle categories, and 906 minor categories. Based on the re-

search objectives, this study filtered the POI data to include only those related to the tourism industry, covering six major tourism elements: catering, accommodation, transportation, sightseeing, shopping, and entertainment. After filtering, the POI data consisted of 13 major categories and 687 minor categories. The data were collected on 10 December 2023.

2.3. Research Methods

The research process in this study is divided into four main steps. First, the NPP/VIIRS and POI data were pre-processed. Second, a Thiessen polygon was created within the boundaries of CZTMA. Third, kernel density analysis was performed on the POI data, and the results were linked to the Thiessen polygon. The POI kernel density analysis was then gridded, normalized, and color-graded. Finally, a two-factor mapping method was employed to couple the NTL data with the POI kernel density analysis (Figure 2).

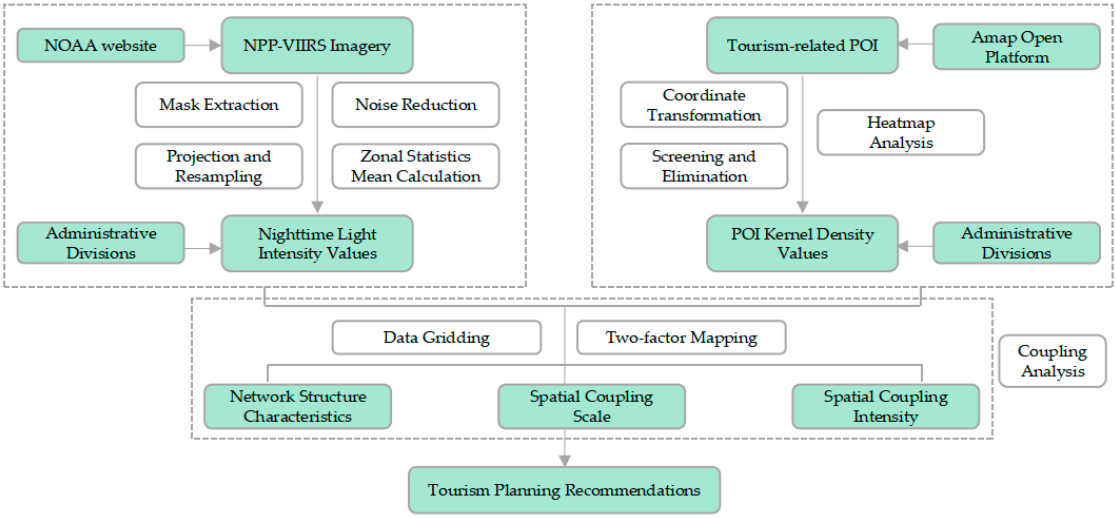


Figure 2. Data collection and analysis process.

2.3.1. Kernel Density Analysis

Kernel density analysis is a spatial density analysis method based on the data density function clustering algorithm [36]. According to the first law of geography, geographical entities are interconnected in space, with closer entities exhibiting stronger relationships. Areas with high POI density typically reflect intense human activity. Kernel density analysis estimates the probability of geographical events occurring within a specific area, primarily analyzing the density of point data [37]. It has broad applications, particularly in studying the spatial distribution of geographical phenomena. In this study, the kernel density analysis of POI data was conducted using the kernel density analysis tool in ArcGIS. The formula is as follows:

$$f(s) = \frac{1}{nh^2} \sum_{i=1}^{n} k\left(\frac{d(s, C_i)}{h}\right) \quad (1)$$

where:

$f(s)$ is the kernel density estimation (KDE) function at spatial position s.

h (bandwidth) refers to the distance decay threshold (3000 m in this study), determined through Silverman's rule of thumb combined with cross-validation tests on POI spatial dispersion patterns. This parameter controls the trade-off between estimation bias and variance—smaller h captures local variations but increases noise, while larger h oversmooths spatial details.

n represents the number of tourism POI points within the circular search window of radius h.
$k(\cdot)$ is the Gaussian kernel function $k(u) = \frac{1}{\sqrt{2\pi}} e^{-\frac{u^2}{2}}$, selected for its non-negative and smooth decay properties to avoid abrupt density discontinuities.
$d(s, C_i)$ indicates Euclidean distance between location s and POI point C_i.

2.3.2. Data Gridding

Gridding is a method in ArcGIS that converts point data into two-dimensional plane data within a specified administrative region. Common grid shapes include triangles, squares, and regular hexagons. According to Christaller's "Central Place Theory", regular hexagons (Thiessen polygons) in spatial topological relations exhibit richer topological characteristics [38]. Additionally, regular hexagonal grids are not constrained by the data format, making them more suitable for analyzing NTL and POI data [39]. This study employs a regular hexagonal grid with a unit area of 1 km², creating a Thiessen polygon grid of 19,574 regular hexagons based on the administrative boundaries of CZTMA. The NTL data and POI kernel density analysis were then vectorized and linked to the grid data. Using the two-factor mapping method, the two datasets were combined to produce an NTL and POI kernel density coupling map.

2.3.3. Two-Factor Combination Mapping

The two-factor mapping method is an intuitive visualization technique that combines two variables to uniformly represent the spatial distribution of a phenomenon within a region [40]. First, the NTL data and POI data were normalized using the fuzzy membership tool in ArcGIS. Next, the datasets were linked to the grid and color-graded using the natural breaks method. Both datasets were classified into high, medium, and low levels. The coupling coordination between them was calculated using the raster calculator, resulting in different coupling coordination degrees. The four primary relationships identified include high POI kernel density with high NTL intensity, low POI kernel density with low NTL intensity, high POI kernel density with low NTL intensity, and low POI kernel density with high NTL intensity.

2.3.4. Multiscale Geographically Weighted Regression (MGWR)

The MGWR model is an advanced method for analyzing spatial heterogeneity, developed based on the generalized additive model [41]. Unlike traditional geographically weighted regression (GWR), the MGWR model allows independent variables to utilize their respective optimal bandwidths, enhancing its explanatory power [42]. The formula is as follows:

$$y_i = \beta_{bw0}(u_i, v_i) + \sum_{j=1}^{k} x_{ij}\beta_{bwj}(u_i, v_i) + \varepsilon_i \quad (2)$$

In the formula, y_i represents the NTL brightness of the ith grid, β_{bw0} is the constant term, (u_i, v_i) are the coordinates of the center point of the ith grid, x_{ij} is the explanatory variable of the model, β_{bwj} denotes the bandwidth used for the regression coefficient of the jth variable, and ε_i is the residual.

2.4. Data Processing

2.4.1. Calculation of Night Light Data

The processing of NTL data involves the following steps: (1) Utilizing spatial analysis extraction tools, the entire CZTMA is designated as the mask range for data extraction. The data management tool is employed to apply the area projection coordinate system, thereby obtaining the image projection raster data. Based on the size of the research area, the image data are spatially resampled to a resolution of 500 m × 500 m. The annual average image is

subsequently derived using the raster calculator. (2) To eliminate background noise and transient light sources, a minimum threshold of 0.3×10^{-9} $W \cdot m^{-2} \cdot sr^{-1}$, as proposed by MA, is applied. Negative values are uniformly set to 0 [43]. Given that Changsha is the most economically developed city within the metropolitan area, the maximum light value observed in Changsha is used as the maximum threshold. Areas exceeding this threshold are considered to have the maximum value. When data errors exceed the threshold, the mean filtering method is employed to calculate the average value of the eight surrounding pixels, which is then assigned as the pixel value for the maximum-value area. (3) A raster attribute data table is created annually using the raster attribute tool. Pixels with an image DN value greater than 0 are extracted using the raster calculator. Statistical analysis of the pixel DN values is conducted via the regional analysis tool to determine the annual NTL total intensity (Total DN, TDN) and the annual NTL total area (Total Area, TA) of the image.

2.4.2. POI Data Screening

The acquired POI data are in the form of point-vector data, containing specific details such as name, type, type code, detailed address, province, city, district/county, GCJ-02 longitude and latitude coordinates, and WGS84 longitude and latitude coordinates. The POI coordinates are uniformly converted to the WGS-1984 geographical coordinate system. A total of 396,307 tourism POI data points were obtained using network crawling tools. After filtering out duplicate, irrelevant, and out-of-scope data, 290,146 POI data points were retained. These include 166,273 catering service points, 14,838 accommodation service points, 45,709 transportation service points, 1008 sightseeing points, 7974 shopping service points, and 54,344 entertainment points (Table 1).

Table 1. Tourism POI in CZTMA.

Category	Quantity/Unit	POI Major Category	POI Middle Category	POI Minor Category	Proportion
Catering Service	166,273	Catering Service	Chinese restaurants, foreign restaurants, fast-food restaurants, casual dining venues, cafes, tea houses, cold-drink stores, cake shops, dessert shops, etc.	Comprehensive restaurants, Northwest cuisine, time-honored brands, hot-pot restaurants, Japanese cuisine, French cuisine restaurants, tea houses, KFC, tea restaurants, Starbucks coffee, etc.	57.31%
Accommodation Service	14,838	Accommodation Service	Hotels, guesthouses	Three-star hotels, four-star hotels, five-star hotels, luxury hotels, youth hostels, economy-chain hotels, accommodation-related services, etc.	5.11%

Table 1. *Cont.*

Category	Quantity/Unit	POI Major Category	POI Middle Category	POI Minor Category	Proportion
Transportation Service	45,709	Transportation Facility Service	Airport-related, railway stations, port terminals, long-distance bus stations, subway stations, light-rail stations, bus stops, taxis, ferry terminals, cableway stations, passenger loading and unloading areas	Airports, railway stations, waiting rooms, ticketing-related, ferry crossings, waiting rooms, passenger ports, airport buses, tourist special-line stations, bus rapid-transit stations, intelligent-rail stations, public parking lots, roadside parking lots, dedicated parking lots, immigration inspection buildings, taxis, ferry terminals, cableway stations, transportation-related services	15.75%
Sightseeing	1008	Scenic Spots	Park squares, scenic spots	Parks, zoos and botanical gardens, aquariums, city squares, world heritage sites, national-level scenic spots, provincial-level scenic spots, memorial halls, temples and Taoist temples, churches, beaches, viewpoints, red-tourism scenic spots	0.35%
Shopping Service	7974	Shopping Service	Shopping malls, convenience stores; home appliance and electronics stores; supermarket;, flower, bird, fish, and insect markets; comprehensive markets; sports goods/cultural goods stores; characteristic commercial streets; clothing, shoe, hat, and leather good stores; personal goods/cosmetics stores	Shopping centers, 7-ELEVEn convenience stores, Gome, digital electronics, Carrefour, Beijing Hualian, Metro, Lotte Mart, Wellcome supermarkets, fruit markets, Nike stores, brand-clothing stores, jewelry and handicraft stores, gift and decoration stores, local-specialty stores, etc.	2.75%

Table 1. *Cont.*

Category	Quantity/Unit	POI Major Category	POI Middle Category	POI Minor Category	Proportion
Entertainment Service	54,344	Life Service	Travel agencies, information consulting centers, ticket offices, photo-printing shops, bathing and massage places, shared facilities	Service centers, hotel inquiries, luggage inquiries, park scenic-spot ticket offices, photo-printing, bathing and massage places, power banks, etc.	18.73%
		Sports and leisure service	Sports fields, golf-related, entertainment venues, vacation and convalescence places, leisure places, theaters, sports and leisure service venues	Comprehensive gymnasiums, ski resorts, KTVs, bars, resorts, beach bathing places, sanatoriums, amusement parks, campsites, cinemas, theaters, concert halls, picking gardens, fishing gardens, etc.	
		Science, Education and Cultural Service	Science, education and cultural places	Museums, exhibition halls, art galleries, science and technology museums, planetariums, cultural palaces	
		Public Facilities	Public toilets	Men's/women's restrooms, disabled restrooms/barrier-free restrooms, baby changing rooms/nursing rooms/mother-and-baby rooms	
Total	290,146				100%

3. Results

3.1. Comparative Analysis of Tourism POI Kernel Density and NTL Intensity

As illustrated in Figure 3, the spatial distribution of tourism points of interest (POIs) generally exhibits a trend of gradual decline from the urban core to the surrounding suburbs. Three high-value areas are identified: the central urban area of Changsha (encompassing Furong District, Yuelu District, and Yuhua District), Yuetang District in Xiangtan, and Hetang District and Tianyuan District in Zhuzhou. The high-value kernel density area in Changsha covers a relatively large expanse, radiating outward continuously, with the primary direction of expansion toward the intersection of Changsha, Zhuzhou, and Xiangtan. The high-value areas in Zhuzhou and Xiangtan are symmetrically distributed along the left and right banks of the Xiangjiang River. These regions, though smaller in extent, radiate outward to surrounding districts and counties. Additionally, the relatively peripheral areas of the Changsha–Zhuzhou–Xiangtan metropolitan region, such as Ningxiang, Liuyang, Liling, Lukou, and Yisuhe, feature sporadic medium-value kernel density points, displaying a multi-point, intermittent distribution. This pattern forms an overall spatial configuration characterized by "dense in the center and sparse on the periphery".

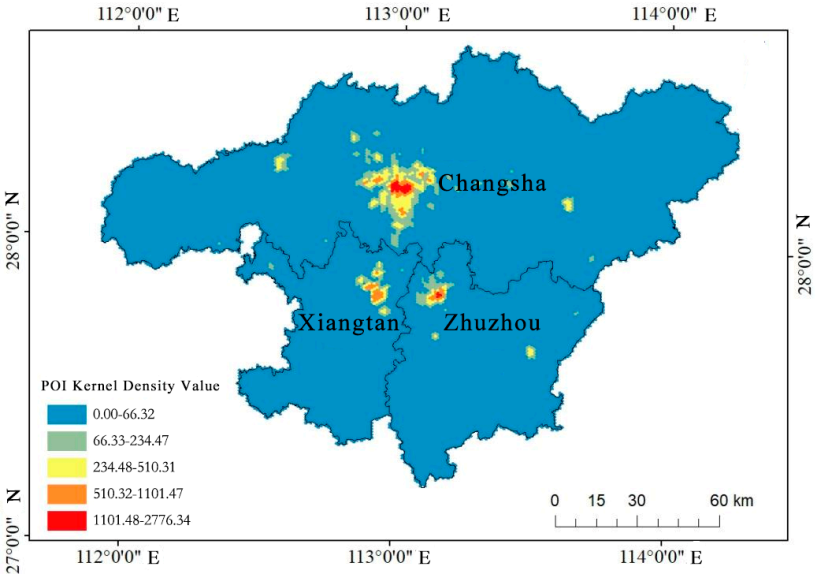


Figure 3. Grid distribution map of tourism POI kernel density in CZTMA.

When the hexagonal grid is overlaid with processed NTL data, the results are shown in Figure 4. The distribution trends of NTL intensity values and tourism POI kernel density values are similar, both exhibiting a radiating pattern from the urban core to the suburbs, with values gradually decreasing. While the three high-value areas remain consistent, the NTL data generate more continuous, centrally clustered regions. The number of high-value centers in Changsha increases, and their surrounding radiation range expands. In Xiangtan and Zhuzhou, the continuous medium- and low-value areas also grow larger. All three high-value areas exhibit a tendency to converge toward the intersection of Changsha, Zhuzhou, and Xiangtan.

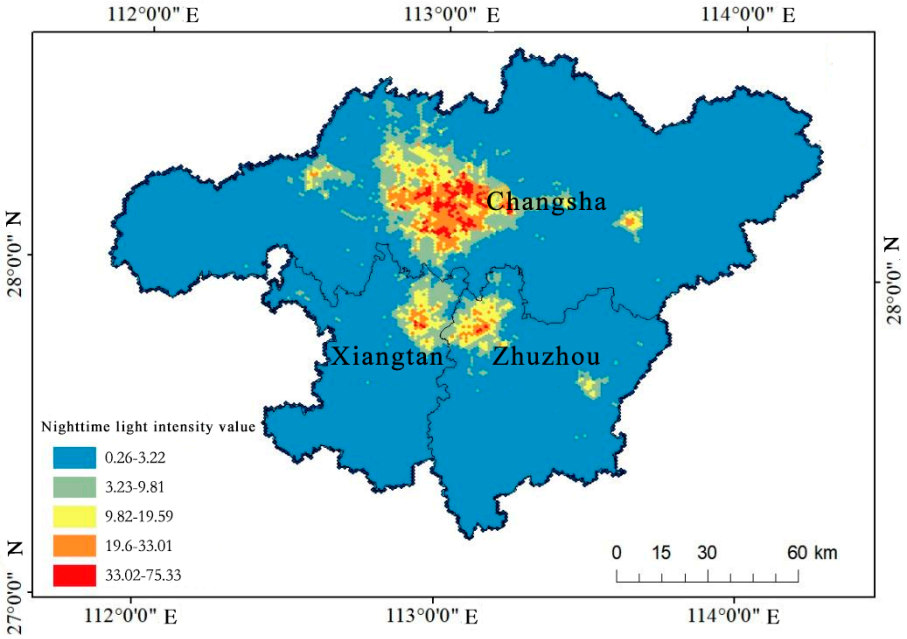


Figure 4. Grid distribution map of NTL intensity in CZTMA.

From a local perspective, the high-value centers of tourism POI kernel density are distributed in a multi-point, intermittent manner, whereas the high-value centers of NTL intensity are distributed in a continuous, clustered pattern, demonstrating a point-to-block-

to-cluster diffusion. In the marginal areas of the metropolitan region, the POI kernel density forms sporadic high-value centers, while the NTL intensity is characterized by large-scale, low-value continuous areas, accompanied by a small number of marginal low-value centers.

3.2. Overall Spatial Distribution of the Coupling Between Tourism POI and NTL

The two types of gridded data were normalized using ArcGIS 10.8 software. Employing the standard-deviation classification method, 1.5 times the standard deviation of the normal distribution was used as the classification criterion. To align with the two-factor mapping method, the data were divided into three levels: high, medium, and low (Table 2). The Thiessen polygon fishnet data were linked to the NTL data and the POI kernel density data, and the coupling between the two datasets was analyzed using the symbol-counting statistical method.

Table 2. Classification of POI data density and NTL intensity.

POI Kernel Density Value			NTL Intensity Value		
Low	Medium	High	Low	Medium	High
<150.4	150.4–805.9	>805.9	<6.52	6.52–26.31	>26.31

As shown in Figure 5, the spatial coupling between tourism POI kernel density and NTL data demonstrates a high degree of spatial coordination. The proportion of hexagonal grids with matching coupling relationships relative to the total number of grids in the study area reached 86.77%. Among these, 495 hexagonal grids exhibited a high–high coupling relationship, 56 grids show a medium–medium coupling relationship, and 16,434 grids display a low–low coupling relationship. Areas with matching coupling relationships generally form a ring-like structure, radiating outward from the intersection of Changsha, Zhuzhou, and Xiangtan. The high–high coupling areas of the two datasets are primarily concentrated along both sides of the Xiangjiang River and in the main urban areas of Changsha–Zhuzhou–Xiangtan. Point-like distributions are also observed in the main urban areas of Ningxiang, Liuyang, and Liling. These regions exhibit high levels of economic development and abundant tourism resources, resulting in elevated POI and NTL values. The medium–medium coupling areas are distributed around the high–high coupling zones, primarily representing transitional areas between urban and suburban regions. The low–low coupling areas are located in suburban and rural areas surrounding the city.

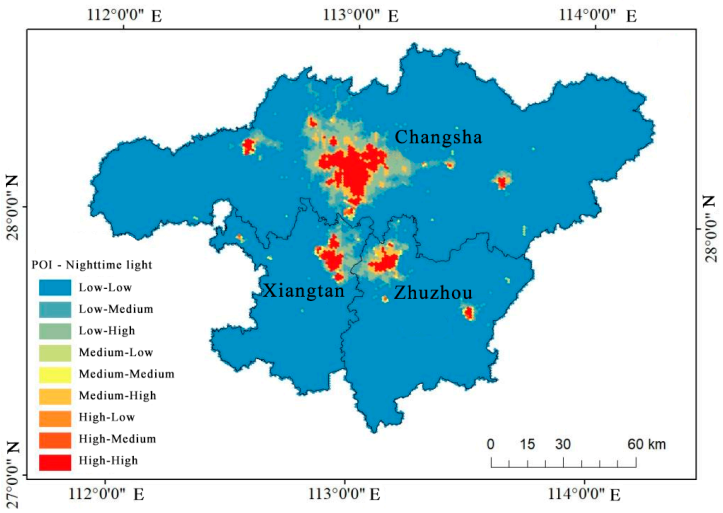


Figure 5. Map of the spatial coupling relationship between tourism POIs and NTL in CZTMA.

3.3. NTL Value Higher than Tourism POI Kernel Density Value

Areas where NTL values exceed tourism POI kernel density values (high–medium coupling, high–low coupling, and medium–low coupling relationships) are primarily distributed outside the high–high and medium–medium coupling zones, forming a ring-like pattern (Figure 6). The high–medium coupling areas are located outside the high–high coupling zones, while the medium–low coupling areas are situated outside the medium–medium coupling zones, mainly in transitional areas between the city center and surrounding villages and towns. Due to their proximity to the city center, and given the saturation of commercial points in the urban core and convenient transportation networks, the number of POIs decreases gradually from the city center outward. However, the light brightness value does not decline significantly due to the light spillover effect. Consequently, the POI value decreases more sharply relative to the light value, resulting in a general trend of declining light values from high to low and forming high–medium coupling areas.

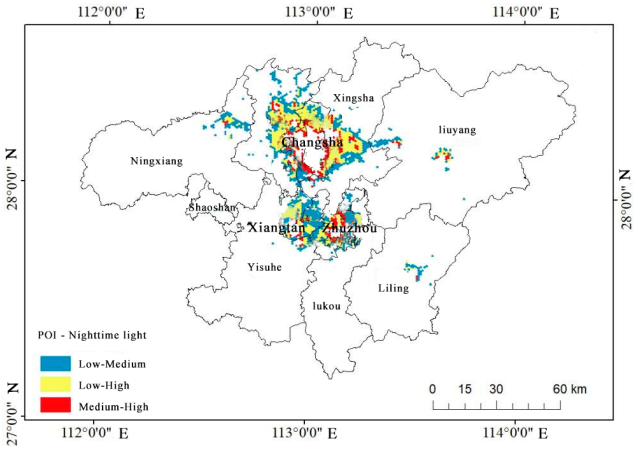


Figure 6. Spatial distribution map of areas where the tourism POI kernel density value is lower than the NTL intensity value.

The high–low coupling areas are found in regions with high light values but few tourism POIs, such as residential areas, industrial parks, government agencies, airports, and other areas with extensive building coverage. Examples include the Sany Heavy Industry Industrial Park and Huanghua International Airport in Xingsha, as well as the government office area in Tianyuan District, Zhuzhou. These areas lack significant tourism POI entities, resulting in NTL values that far exceed POI values.

The medium–low coupling areas are predominantly located in suburban regions, far from the city center. These areas are typically characterized by factories, transportation facilities, and logistics industries, which are associated with low land prices and minimal pollution. For instance, the Shifeng District Industrial Park in Zhuzhou hosts a large number of factories and affiliated institutions, driving the development of transportation and logistics industries and ultimately forming medium–low coupling areas.

3.4. NTL Value Lower than Tourism POI Kernel Density Value

Areas where NTL values are lower than tourism POI kernel density values are less common. Overall, medium–high and low–medium coupling areas dominate, while low–high coupling areas are rare. As shown in Figure 7, the high population density in the central urban area results in tourism POI density exceeding the light threshold, forming medium–high coupling areas. Examples include Wuyi Avenue in Changsha, Jianshe South Road in Zhuzhou, and Shaoshan Road in Xiangtan. The low–medium coupling areas are sparsely distributed in the main urban area and are primarily found in less-developed

fringe areas, as well as urban parks or green spaces transitioning from the city center to the suburbs. Examples include Xiangfu Cultural Park in Changsha, Tianma Mountain Park, Yuhu Park in Xiangtan, and Shaofeng Park in Shaoshan.

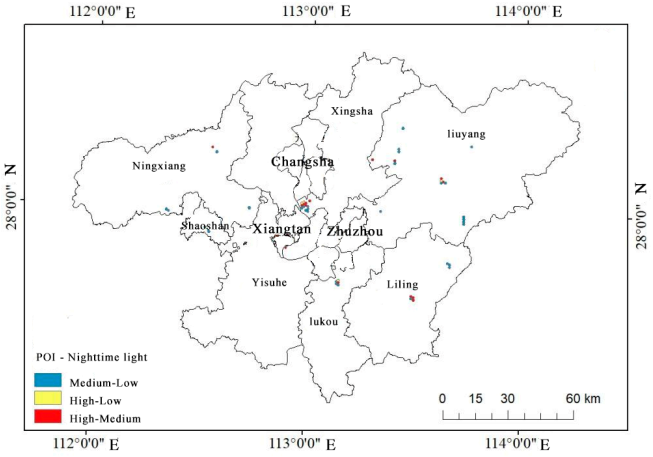


Figure 7. Spatial distribution map of areas where the tourism POI kernel density value is lower than the NTL intensity value.

3.5. Correlation Between Different Types of Tourism Spaces and NTL Values

The closer the Multiscale Geographically Weighted Regression (MGWR) bandwidth is to the global scale, the greater the influence of the explanatory variable on NTL brightness at a broader or global scale [44]. Conversely, a smaller bandwidth indicates that the explanatory variable affects the average brightness value locally or within a smaller range. Based on the calculations from Model (2), the MGWR bandwidth ranges between 69 and 1993, indicating significant variation in the scale of influence (Table 3).

Table 3. Descriptive statistical results of regression coefficients of classical GWR and MGWR models.

Variable	GWR Bandwidth	MGWR					
		Bandwidth	Mean	Standard Deviation	Minimum	Median	Maximum
catering	106	1976	0.050	0.000	0.050	0.050	0.051
accommodation	106	1982	0.066	0.000	0.064	0.066	0.067
transportation	106	128	0.534	0.260	0.193	0.508	1.406
sightseeing	106	69	0.082	0.373	−0.977	0.016	2.866
shopping	106	1993	−0.074	0.000	−0.075	−0.074	−0.072
entertainment	106	1993	0.058	0.000	0.056	0.058	0.059

The distribution factor of shopping spaces has a negligible and negative correlation. The coefficient values range from −0.074 to −0.072, with an average of −0.074. The coefficient exhibits a gradual decline from the center to the periphery of the study area, with the negative impact intensifying outward. The distribution factor of accommodation spaces shows a positive but insignificant correlation. The coefficient values range from 0.064 to 0.067, with an average of 0.066, displaying a circular-layered decline from the center to the periphery. The MGWR regression results for shopping, catering, and entertainment factors approximate the global bandwidth, indicating local characteristics. Although some spatial variation exists, the changes are not significant, and the coefficients remain relatively stable across space. The distribution factor of transportation spaces is positively correlated with NTL brightness. The regression coefficient values range from 0.193 to 1.406, with an average of 0.534. In terms of absolute value, its impact is moderate. The number of transportation POIs in the grid is fixed, and the rate of decline in NTL intensity from the

city center to the periphery is less pronounced than that of transportation POIs, generally showing an increasing trend from the center outward. The regression coefficient for the distribution factor of sightseeing spaces transitions from positive to negative, moving from multiple high-value centers to the periphery. The coefficient values range from −0.977 to 2.866, with an average of 0.082. In absolute terms, its impact is the most significant. The results suggest that, within a localized range, sightseeing spaces exert a substantial influence on NTL brightness, with notable spatial heterogeneity.

4. Discussion

By gridding and normalizing the POI and NTL data of CZTMA and conducting a coupling analysis, this study explores the characteristics of the spatial structure of tourism within the region. The findings provide a critical decision-making framework for sustainable urban tourism development by revealing the spatial interaction mechanisms, serving as an early warning system for detecting unsustainable expansion patterns.

4.1. Refined Identification of Tourism Development Centers

Compared to existing studies based on statistical data, this paper overcomes the limitations of administrative units by utilizing NTL data combined with tourism POI data. This approach identifies the main centers of tourism development in CZTMA at a more refined scale. Additionally, it analyzes the characteristics of the spatial structure of tourism from multiple perspectives, including the functional structure of the main centers, spatial correlation measurement, and the service range of these centers.

The results reveal that tourism development in CZTMA is concentrated in the central region, with weaker development in the eastern and western parts. The intersection area of the three cities shows a clear trend of enhancement, indicating overall unbalanced development. The kernel density of tourism POIs in marginal areas such as Ningxiang, Liuyang, Liling, and Yisuhe are nearly zero, suggesting that the tourism industry in these areas is not dominant and requires the driving force of strong tourism attractions. Notably, high–high spatial coupling zones account for 2.52% of the total study area, exceeding the values reported in the Shanghai, Fuzhou, and Changchun metropolitan areas [15,44]. This disparity highlights intensified spatial polarization within central China's newly metropolitan areas, potentially attributable to asymmetric resource allocation mechanisms under regional development policies. In the future, the tourism industry of CZTMA should aim to balance regional development, further optimize the spatial layout of tourism, strengthen Changsha's leading role, leverage the comparative advantages of Zhuzhou and Xiangtan, and jointly build a tourism spatial pattern characterized by complementary strengths and high-quality development. More specifically, the local government could establish a tourism development fund allocating some of Changsha's tourism revenue to subsidize infrastructure in peripheral counties (such as Ningxiang and Liuyang), following the EU's structural fund model for regional cohesion [13]. Consequently, policymakers can stimulate job creation, diversify local economies, and reduce migration pressures on urban centers—key tenets of SDG 8. Furthermore, a cross-city tourism commission with authority should be created in order to coordinate attraction ticket pricing, transportation links, and marketing budgets across municipal boundaries, addressing current fragmentation issues.

4.2. Effectiveness of the Combined POI and NTL Data Method

This study validates the effectiveness of the method combining POI data and NTL remote sensing data for identifying the tourism spatial structure of metropolitan areas. This approach provides a new perspective for evaluating urban tourism development. Unlike single NTL data, POI data incorporate characteristics related to metropolitan boundaries,

such as the relationship between regional scale and human activities, offering a more comprehensive representation of tourism's spatial structures.

The high–high coupling areas are primarily distributed in the centers of three cities and extend to the urban periphery, consistent with previous studies on CZTMA [45]. Compared to the single-center model dominant in European metropolitan areas [11], the multi-center identification better captures the transitional spatiality of Chinese urban agglomerations. The intersection area of the three cities is surrounded by three high–high coupling zones (Figure 8). In the future, this area should be designated as the metropolitan's "Urban Central Park", capitalizing on the Xiangjiang River's hydrological network, surrounding mountain ranges, and arterial transportation corridors. Development priorities must emphasize establishing interconnected nature reserves, suburban park clusters, urban green spaces, and multi-functional greenway systems to create an integrated ecological matrix. Through protective development, local governments could promote green industries such as scientific and technological innovation, creative design, health and wellness, and sports. This would create several green ecological corridors extending to surrounding counties and cities, establishing the urban green heart and ecological security barrier of the metropolitan area. This approach not only preserves biodiversity but also aligns with SDG 11's emphasis on sustainable urban ecosystems.

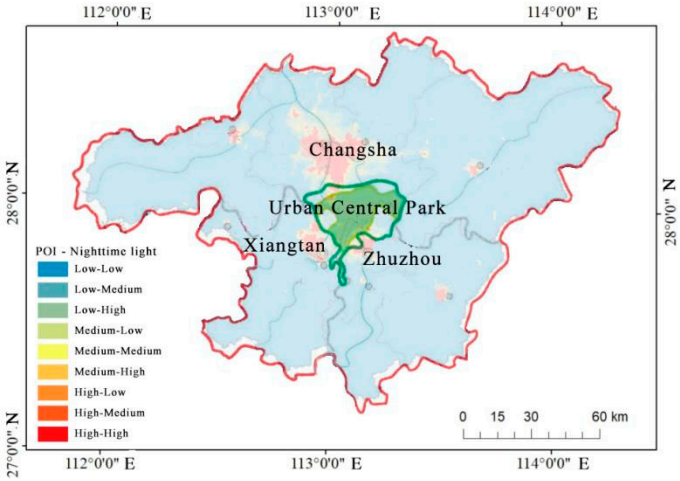


Figure 8. The ideal location of the "Urban Central Park of CZTMA".

4.3. Spatial Distribution Coupling Heterogeneity

In terms of spatial distribution coupling heterogeneity, medium–high and low–medium coupling areas are mainly distributed in high-density residential areas, industrial parks, government office zones, and less-developed suburban regions. These areas could benefit from the planning of more outdoor recreational spaces, such as urban green spaces, neighborhood parks, and special-themed gardens. These spaces would not only serve as excellent venues for citizens to travel and relax but would also play a crucial role in the urban ecosystem by mitigating the urban heat island effect. Consequently, the local government could implement effective measures to increase POI density in these zones, such as mandating the provision of visitor service centers within specific scope, enforcing park-green space coverage requirements, and requiring new residential developments to allocate some land area for cultural-tourism facilities.

Meanwhile, those areas where the tourism POI kernel density value exceeds the NTL intensity value are primarily located in characteristic small towns such as Huaminglou Town, Daweishan Town, Huitang Town, and Yisuhe Town. These areas are rich in tourism resources and feature numerous scenic spots. However, inadequate public infrastructure, insufficient supporting service facilities, and the homogenization of tourism products have

resulted in few overnight tourists, short stay durations, and the limited realization of comprehensive tourism benefits. The tourism homogeneity issue in small towns mirrors challenges observed in Isfahan's heritage tourism clusters [16], indicating a global need for differentiated product strategies in peri-urban areas. Municipal authorities should allocate targeted subsidies to upgrade nightlife amenities, boosting tourist expenditure and stay duration. Leveraging regional assets, towns must strategically develop unique tourism products while strengthening infrastructure and public services to meet diverse visitor needs. For instance, Huaminglou Town may specialize in cultural heritage tourism through its historical architecture preservation; Daweishan Town in eco-wellness tourism, capitalizing on mountainous forest resources; and Huitang Town in agritourism, integrating leisure farming experiences with rural hospitality. Such mechanisms can foster synergistic tourism clusters that maximize regional resource efficiency while advancing the SDGs' "leave no one behind" agenda.

In the future, a tiered governance approach should be drawn from the adaptive management framework in metropolitan planning, where policy instruments are dynamically adjusted based on real-time NTL and POI coupling monitoring through our proposed methodology.

4.4. Limitations and Future Research Directions

This study has some limitations. First, the tourism POI data are sourced solely from the Amap Open Platform, resulting in a single data source. Future research could implement a multi-source data integration framework incorporating platforms such as Baidu Map and Tencent Map. Advanced data fusion techniques (e.g., spatial-temporal matching algorithms and entity resolution methods) could be employed to harmonize heterogeneous data formats across platforms, thereby enhancing dataset comprehensiveness and spatial accuracy. Second, the timeliness of POI data presents methodological challenges, as most Chinese Internet electronic maps implement daily updates to maintain accuracy, thereby impeding the acquisition of historical tourism POI records. Future studies could develop a distributed web-crawling system with periodic archival storage capabilities to systematically capture and preserve daily POI snapshots. Furthermore, they could collaborate with commercial map platforms through research partnerships to obtain privileged access to version-controlled historical POI repositories. Such methodological advancements would enable more robust temporal analyses spanning 5–10 year periods, significantly improving the predictive capacity of tourism–economic development models.

5. Conclusions

The main conclusions of this study are as follows: (1) Based on NTL maps and POI kernel density analysis, the study finds that tourism POI kernel density in CZTMA exhibits a multi-point distribution with strong geographical concentration. High-kernel-density regions centered on downtown areas radiate outward to surrounding scenic spots. The NTL intensity value (TDN) shows a trend of first increasing and then decreasing, with the light area (TA) of the three cities exhibiting continuous expansion. The brightness value gradually decreases as the city center expands outward. (2) The spatial coupling of NTL data and tourism-related POIs in CZTMA demonstrates a high degree of homogeneity. Regions with matching coupling relationships generally form a ring-shaped structure. The coupling relationship is closely related to regional economic development levels and land use types. (3) NTL brightness is the result of multiple factors, and the relationships between different types of tourism spaces and NTL brightness vary. Among these, the influence of scenic spots transitions from positive to negative from high-value areas outward, exhibiting the strongest impact. This spatially explicit approach to tourism–environment

interaction analysis fundamentally enhances our capacity to implement the "monitorable-reportable-verifiable" framework required by international sustainable tourism protocols while providing Chinese megacity clusters with a replicable model for achieving coordinated development between tourism growth and urban sustainability.

Author Contributions: Conceptualization, J.W. and Q.Z.; methodology, J.W. and Q.Z.; software, J.W.; project administration, Q.Z.; validation, J.W., Q.Z. and J.W.; visualization, Z.L.; original draft writing, J.W. and Z.L.; writing review and editing, J.W. and Z.L.; funding acquisition, Q.Z.; supervision, Q.Z. All authors have read and agreed to the published version of the manuscript.

Funding: This research was funded by the Social Science Fund Project of Hunan Province: Research on the Evolution and Optimization of the Recreational Network Space in the Green Heart Area of the Changsha–Zhuzhou–Xiangtan Metropolitan Area, grant number 23JD024.

Institutional Review Board Statement: Not applicable.

Informed Consent Statement: Not applicable.

Data Availability Statement: Please contact the authors via email for the data.

Conflicts of Interest: The authors declare no conflicts of interest.

References

1. Beaudry, P.; Mark, D.; Lewis, E. Should the personal computer be considered a technological revolution? Evidence from US metropolitan areas. *J. Polit. Econ.* **2010**, *118*, 988–1036. [CrossRef]
2. Li, X.; Zhou, W.; Ouyang, Z.; Xu, W.; Zheng, H. Spatial pattern of greenspace affects land surface temperature: Evidence from the heavily urbanized Beijing metropolitan area, China. *Landsc. Ecol.* **2012**, *27*, 887–898. [CrossRef]
3. Nasri, A.; Zhang, L. The analysis of transit-oriented development (TOD) in Washington, DC and Baltimore metropolitan areas. *Transp. Policy* **2014**, *32*, 172–179. [CrossRef]
4. Zhang, H. Metro and urban growth: Evidence from China. J. *Transp. Geogr.* **2020**, *85*, 102732. [CrossRef]
5. Nasri, A.; Zhang, L. Assessing the impact of metropolitan-level, county-level, and local-level built environment on travel behavior: Evidence from 19 US urban areas. *J. Urban Plan. Dev.* **2015**, *141*, 04014031. [CrossRef]
6. Yang, Y.; Fik, T. Spatial effects in regional tourism growth. *Ann. Tour. Res.* **2014**, *46*, 144–162. [CrossRef]
7. Zhong, C.; Arisona, S.M.; Huang, X.; Batty, M.; Schmitt, G. Detecting the dynamics of urban structure through spatial network analysis. *Int. J. Geogr. Inf. Sci.* **2014**, *28*, 2178–2199. [CrossRef]
8. Hall, C.M.; Page, S.J. *The Geography of Tourism and Recreation: Environment, Place and Space*; Routledge: London, UK, 2014; pp. 96–102.
9. Dredge, D.; Jamal, T. Progress in tourism planning and policy: A post-structural perspective on knowledge production. *Tour. Manag.* **2015**, *51*, 285–297. [CrossRef]
10. Meijers, E.J.; Burger, M.J. Spatial structure and productivity in US metropolitan areas. *Environ. Plan. A* **2010**, *42*, 1383–1402. [CrossRef]
11. Vasanen, A. Functional polycentricity: Examining metropolitan spatial structure through the connectivity of urban sub-centres. *Urban Stud.* **2012**, *49*, 3627–3644. [CrossRef]
12. Wang, T.; Li, H.; Huang, Y. The complex ecological network's resilience of the Wuhan metropolitan area. *Ecol. Indic.* **2021**, *130*, 108101. [CrossRef]
13. Albalate, D.; Bel, G. Tourism and urban public transport: Holding demand pressure under supply constraints. *Tour. Manag.* **2010**, *31*, 425–433. [CrossRef]
14. Scott, J.W. A networked space of meaning? Spatial politics as geostrategies of European integration. *Space Polity* **2002**, *6*, 147–167. [CrossRef]
15. Huang, J.; Xu, Y.; Hu, G.; He, Y.; Zhao, M. Analysis of Borrowing Scale of Metropolitan Network Externalities: A Case Study of the Shanghai Metropolitan Area. *Urban Dev. Stud.* **2024**, *31*, 16–23. (In Chinese)
16. Ghaed, S.; Daneshmandi, N. Analysis of urban tourism spatial pattern (case study: Urban tourism space of Isfahan city). *Hum. Geogr. Res.* **2018**, *50*, 945–961.
17. Gao, P.; Xi, J. Research on the Spatial Structure and Complex Characteristics of Tourism Destination Network—A Case Study of Yesanpo Tourism Destination. *J. Nat. Resour.* **2018**, *33*, 85–98.
18. Li, Y.; Xiao, L.; Ye, Y.; Xu, W.; Law, A. Understanding tourist space at a historic site through space syntax analysis: The case of Gulangyu, China. *Tour. Manag.* **2016**, *52*, 30–43. [CrossRef]

19. Yang, Z.; Li, T. Does high-speed rail boost urban tourism economy in China? *Curr. Issues Tour.* **2020**, *23*, 1973–1989. [CrossRef]
20. Wen, H.; Tao, Y. Polycentric urban structure and housing price in the transitional China: Evidence from Hangzhou. *Habitat Int.* **2015**, *46*, 138–146. [CrossRef]
21. Lou, G.; Chen, Q.; He, K.; Zhou, Y.; Shi, Z. Using nighttime light data and POI big data to detect the urban centers of Hangzhou. *Remote Sens.* **2019**, *11*, 1821. [CrossRef]
22. Yu, J.; Meng, Y.; Zhou, S.; Zeng, H.; Li, M.; Chen, Z.; Nie, Y. Research on spatial delineation method of urban-rural fringe combining poi and nighttime light data—Taking Wuhan city as an example. *Int. J. Environ. Res. Public Health* **2023**, *20*, 4395. [CrossRef] [PubMed]
23. Wei, W.; Chen, D.; Zhang, X.; Ma, L.; Xie, B.; Zhou, J.; Wang, M.; Wei, X.; Yang, S.; Yan, P. Estimation of carbon emissions from different industrial categories integrated nighttime light and POI data—A case study in the Yellow River Basin. *J. Environ. Manag.* **2024**, *370*, 122418. [CrossRef]
24. Wang, N.; Liu, Y.; Wang, J.; Qian, X.; Zhao, X.; Wu, J.; Wu, B.; Yao, S.; Fang, L. Investigating the potential of using POI and Nighttime Light data to map urban road safety at the micro-level: A case in Shanghai, China. *Sustainability* **2019**, *30*, 4739. [CrossRef]
25. Yan, G.; Zou, L.; Liu, Y. The Spatial Pattern and Influencing Factors of China's Nighttime Economy Utilizing POI and Remote Sensing Data. *Appl. Sci.* **2024**, *14*, 400. [CrossRef]
26. Chen, Z.; Xu, W.; Zhao, Z. The Assessment of Industrial Agglomeration in China Based on NPP-VIIRS Nighttime Light Imagery and POI Data. *Remote Sens.* **2024**, *16*, 417. [CrossRef]
27. Zheng, Y.; Tang, L.; Wang, H. An improved approach for monitoring urban built-up areas by combining NPP-VIIRS nighttime light, NDVI, NDWI, and NDBI. *J. Clean. Prod.* **2021**, *328*, 129488. [CrossRef]
28. Ou, J.; Liu, X.; Li, X.; Li, M.; Li, W. Evaluation of NPP-VIIRS Nighttime Light Data for Mapping Global Fossil Fuel Combustion CO2 Emissions: A Comparison with DMSP-OLS Nighttime Light Data. *PLoS ONE* **2015**, *10*, e0138310. [CrossRef]
29. Wang, Z.; Zheng, J.; Han, C.; Lu, B.; Yu, D.; Yang, J.; Han, L. A comprehensive assessment approach for multiscale regional economic development: Fusion modeling of nighttime lights and OpenStreetMap data. *Geogr. Sustain.* **2025**, *6*, 100230. [CrossRef]
30. Tang, C. Improvement of urban construction land extraction method based on NPP-VIIRS nighttime light data and landsat-8 data: A case study of Guangzhou city. *Geomat. Spat. Inf. Technol.* **2017**, *40*, 69–73.
31. Fu, C.; Tu, X.; Huang, A. Identification and characterization of Production–living–ecological space in a central urban area based on POI data: A case study for Wuhan, China. *Sustainability* **2021**, *13*, 7691. [CrossRef]
32. Lu, C.; Pang, M.; Zhang, Y.; Li, H.; Lu, C.; Tang, X.; Cheng, W. Mapping urban spatial structure based on poi (point of interest) data: A case study of the central city of Lanzhou, China. *Int. J. Geo-Inf.* **2020**, *9*, 92. [CrossRef]
33. Zhao, F.; Chu, C.; Liu, R.; Peng, Z.; Du, Q.; Xie, Z.; Sun, Z.; Zeng, H.; Xia, J. Assessing Light Pollution Using POI and Luojia1-01 Night-Time Imagery From a Quantitative Perspective at City Scale. *IEEE J. Sel. Top. Appl. Earth Obs. Remote Sens.* **2021**, *14*, 7544–7556.
34. Ouyang, X.; Xu, J.; Li, J.; Wei, X.; Li, Y. Land space optimization of urban-agriculture-ecological functions in the Changsha-Zhuzhou-Xiangtan Urban Agglomeration, China. *Land Use Policy* **2022**, *117*, 106112. [CrossRef]
35. Miller, S.; Straka, W.; Mills, S.; Elvidge, C.; Lee, T.; Solbrig, J.; Walther, A.; Heidinger, A.; Weiss, S. Illuminating the capabilities of the Suomi national polar-orbiting partnership (NPP) visible infrared imaging radiometer suite (VIIRS) day/night band. *Remote Sens.* **2013**, *5*, 6717–6766. [CrossRef]
36. Yu, W.; Ai, T.; Shao, S. The analysis and delimitation of Central Business District using network kernel density estimation. *J. Transp. Geogr.* **2015**, *45*, 32–47. [CrossRef]
37. Wenhao, Y.; Tinghua, A. The visualization and analysis of POI features under network space supported by kernel density estimation. *Acta Geod. Cartogr. Sin.* **2015**, *44*, 82.
38. Getis, A.; Getis, J. Christaller's central place theory. In *A Geography of Urban Places*; Routledge: London, UK, 2014; pp. 68–72.
39. Tang, X.; Liu, Y.; Pan, Y. An evaluation and region division method for ecosystem service supply and demand based on land use and POI data. *Sustainability* **2020**, *12*, 2524. [CrossRef]
40. Jang, S.; Choi, H.; Park, S.; Jaekal, E.; Lee, G.; Cho, Y.; Choi, K. A two-factor model better explains heterogeneity in negative symptoms: Evidence from the positive and negative syndrome scale. *Front. Psychol.* **2016**, *12*, 707. [CrossRef]
41. Fotheringham, A.; Yang, W.; Kang, W. Multiscale geographically weighted regression (MGWR). *Ann. Am. Assoc. Geogr.* **2017**, *107*, 1247–1265. [CrossRef]
42. Shabrina, Z.; Buyuklieva, B.; Ng, M. Short-term rental platform in the urban tourism context: A geographically weighted regression (GWR) and a multiscale GWR (MGWR) approaches. *Geogr. Anal.* **2021**, *53*, 686–707. [CrossRef]
43. Ma, T.; Zhou, C.; Pei, T.; Haynie, S.; Fan, J. Responses of Suomi-NPP VIIRS-derived nighttime lights to socioeconomic activity in China's cities. *Remote Sens. Lett.* **2014**, *5*, 165–174. [CrossRef]

44. Wu, Z.; Wei, X.; He, X.; Gao, W. Identifying Urban Built-Up Areas Based on Spatial Coupling between Nighttime Light Data and POI: A Case Study of Changchun. *Buildings* **2023**, *14*, 19. [CrossRef]
45. Zheng, Z. Spatial structure of the Changsha–Zhuzhou–Xiangtan urban agglomeration based on dynamic simulation analysis. *J. Urban Plan. Dev.* **2015**, *141*, 04014035. [CrossRef]

Disclaimer/Publisher's Note: The statements, opinions and data contained in all publications are solely those of the individual author(s) and contributor(s) and not of MDPI and/or the editor(s). MDPI and/or the editor(s) disclaim responsibility for any injury to people or property resulting from any ideas, methods, instructions or products referred to in the content.